Journal of the Korea Concrete Institute
Vol.17 No.4, pp.645~654, August, 2005

Nonlinear Analysis of Reinforced and Prestressed Concrete Shells Using Layered Elements with Drilling DOF

Tae-Hoon Kim[1], Jung-Ho Choi[2], Woon-Hak Kim[2], and Hyun Mock Shin[3]*

[1]*Civil Engineering Research Team, Daewoo Institute of Construction Technology, Suwon, 440-210, Korea*
[2]*Dept. of Civil Engineering, Hankyong National University, Ansung, 456-240, Korea*
[3]*Dept. of Civil and Environmental Engineering, Sungkyunkwan University, Suwon, 440-746, Korea*

(Received, December 10, 2004, Accepted, July 30, 2005)

Abstract

This paper presents a nonlinear finite element procedure for the analysis of reinforced and prestressed concrete shells using the four-node quadrilateral flat shell element with drilling rotational stiffness. A layered approach is used to discretize, through the thickness, the behavior of concrete, reinforcing bars and tendons. Using the smeared-crack method, cracked concrete is treated as an orthotropic nonlinear material. The steel reinforcement and tendon are assumed to be in a uni-axial stress state and to be smeared in a layer. The constitutive models, which cover the loading, unloading, and reloading paths, and the developed finite element procedure predicts with reasonable accuracy the behavior of reinforced and prestressed concrete shells subjected to different types of loading. The proposed numerical method for nonlinear analysis of reinforced and prestressed concrete shells is verified by comparison with reliable experimental results.

***Keywords** : nonlinear finite element procedure, drilling rotational stiffness, layered approach, smeared-crack*

1. Introduction

In recent years, reinforced and prestressed concrete shells have been widely applied to underground tanks, nuclear waste containers, and offshore structures. Nonlinear finite element analysis of such structures has become increasingly important because it is generally not possible to determine deformation and failure behavior by conventional procedures, and experimental studies on these structures are very expensive.

Considerable effort has been made to develop suitable nonlinear finite element analysis method for application to reinforced and prestressed concrete shells [1, 2]. Much of this research has focused on developing specialized element and efficient solution algorithms, with insufficient attention to the implementation of realistic constitutive models that accurately predict the behavior of concrete shells[3].

In the present study, models were developed to address material nonlinearity by incorporating tensile, compressive and shear models for cracked concrete, in addition to including model for the reinforcing bars and tendons, which uses the smeared crack approach. The impetus in developing these models was to represent time dependent behavior by proper theoretical representation of the material parameters.

The primary objective of this study was to develop a new finite element formulation for the nonlinear analysis of concrete shell structures. In order to analyze reinforced and prestressed concrete shells with highly nonlinear behavior, the layer method was introduced, assuming that several thin plane stress elements are layered in the direction of thickness. Each layer consists of four-node flat shell elements. The flat shell element was developed by combining a membrane element with drilling degree of freedom and a plate-bending element. Thus, the developed element possesses six degrees of freedom (DOF) per node, allowing for an easy connection to other types of finite elements that have 6-DOFs per node, a three-dimensional beam-column element, etc., and providing a much improved, more robust analysis procedure than currently exists[4].

* *Corresponding author*
E-mail address: hmshin@skku.ac.kr
©2005 by Korea Concrete Institute

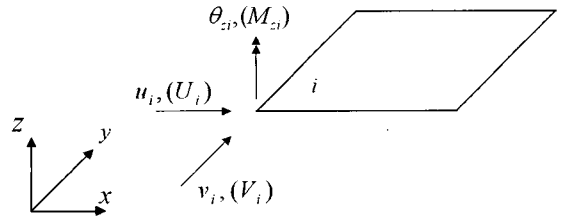

(a) Plane-membrane actions and deformations

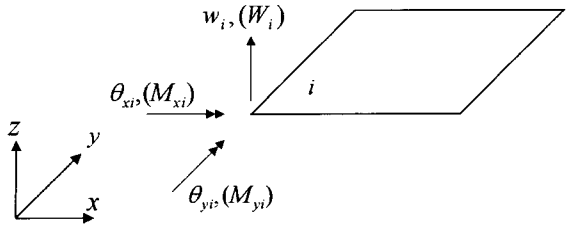

(b) Bending actions and deformations

Fig. 1 Flat-shell element subjected to plane-membrane and bending actions

The efficiency of the numerical method, and even its actual capacity to be used repeatedly for practical problems, mainly follows from the technique adopted to perform the complete geometric description. Their comparisons with available experimental or analytical results from other authors have shown both the satisfactory efficiency and reliability of the method. However, a lack of experimental studies about reinforced and prestressed concrete shells has been found, meaning that experimental research is still needed regarding future verification and extension.

2. Finite element formulation

Presented herein is a finite element formulation for the analysis of reinforced and prestressed concrete shells using a four-node quadrilateral thin flat shell finite element with 6-DOFs per node. The sixth DOF is obtained by combining a membrane element with a normal rotation, θ_z, the so-called drilling degree of freedom, and a discrete Kirchhoff plate element[4]. Flat shell finite elements may be formulated through the use of a variational formulation that includes an independent rotation field for the drilling degree of freedom. These modeling assumptions are shown in Fig. 1.

The element had to be based on a three-dimensional elastic formulation. In order to analyze reinforced and prestressed concrete shells with nonlinear behavior, the layer method was used, assuming that several thin plane stress elements are layered in the direction of thickness. In the layered element formulation, the shell is divided into several paneled layers and two-dimensional constitutive models were applied to take into account material nonlinearities.

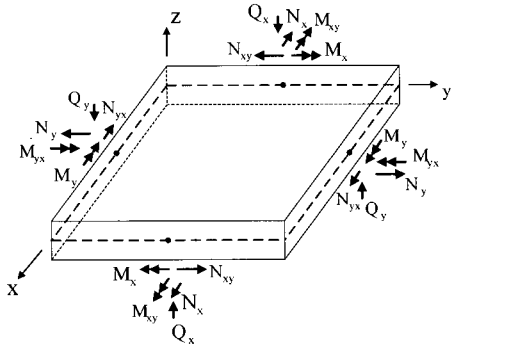

(a) Forces acting on reinforced and prestressed concrete shells

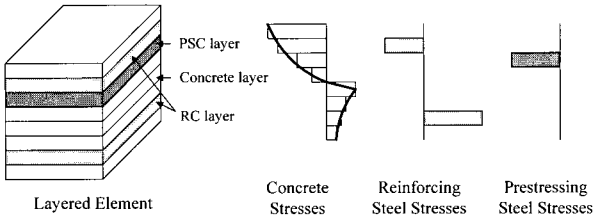

(b) Layered element

Fig. 2 Shell element

Fig. 2 illustrates the layered element and forces acting on the shells. Integration through the thickness of element was achieved through layered-element formulation. In the depth of its mid-surface, one-integration point was used for each layer of panel. Each layer was classified as either a plain concrete layer or a reinforced and prestressed concrete layer, where the reinforcing bars and tendons were smeared in the layer, as shown in Fig. 2. Most of the formulations presented up to now which include prestressing have been developed as an extension of existing models for the analysis of reinforced concrete structures, and agree in their main features. However, so far this application has found a practical limitation in the lack of available experimental results to be used for the verification.[5]

In this study, prestressing is considered as an initial unbalanced stress and an equivalent load system is evolved and applied in the opposite direction to find the deformations and stresses in the structure due to prestressing. An automatic procedure has been also developed that, using a set of analytical expressions as primordial data to describe the shell and the courses of the tendons, later generates a global geometric interpolation. The interpolation of the tendon courses is dependent to the isoparametric interpolation of a shell element. This application to concrete shell structures has one of its more important aspects in the need to minimize the input data preparation for the complete definition of the geometry of the problem, including the shell middle surface and the space curves that refer the axis of prestressing tendons.

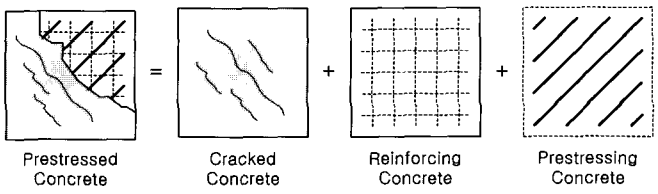

Fig. 3 Shell element model

Prestressing tendons with arbitrary tendon profiles are modeled with a number of piecewise linear tendon segments defined by tendon points. Each tendon point is associated with a node, to which its displacements are rigidly constrained. The global coordinates of the tendon points may be input directly or may be generated automatically using a parametric generation scheme. The prestressing tendons may be stressed, restressed or removed at any stage of the solution.

3. Nonlinear material model

The nonlinear material model for the reinforced and prestressed concrete is composed of models to characterize the behavior of the concrete, in addition to models for characterizing the reinforcing bars and tendons (see Fig. 3).

Models for concrete may be divided into models for uncracked concrete and cracked concrete. The basic model adopted for crack representation is a non-orthogonal fixed-crack method of the smeared crack concept, which is widely known to be a model for crack representation. This approach is practical for cyclic loads where the load history needs to be recorded. This section includes summaries of the material models used in the analysis. A full description of the nonlinear material model for reinforced concrete is given by Kim et al.[4]

3.1 Model for uncracked and cracked concrete

The widely used elasto-plastic and fracture model for the biaxial state of stress proposed by Maekawa and Okamura[6] is used as the constitutive equation for the uncracked concrete. For uncracked concrete, the nonlinearity, anisotropy, and strain softening effects are expressed independently of the loading history.

After concrete cracks, the behavior becomes anisotropic in the crack direction. The stress-strain relations are modeled by being decomposed in directions parallel to, along and normal to cracks, respectively. Thus, the constitutive law adopted for the cracked concrete consists of tension stiffening, compression stiffness and shear transfer models.

Cracked concrete may resist a certain amount of tensile stress normal to the cracked plane because of the bond effect between the concrete and the reinforcing bars. A refined tension stiffening model is obtained by transforming the tensile stresses of concrete into the component normal to the crack, and improved accuracy is expected, especially when the reinforcing ratios in orthogonal directions are significantly different and when the reinforcing bars are distributed only in one direction. For the tension stiffening model for unloading and reloading, the model proposed by Shima et al.[7] is basically used.

A modified elasto-plastic fracture model is used to describe the compressive behavior of concrete struts in between cracks in the direction of the crack plane. The model describes the degradation in compressive stiffness by modifying the fracture parameter in terms of the strain perpendicular to the crack plane. The cyclic load causes damage to the inner concrete and energy is dissipated during the unloading and reloading processes. This behavior is considered in the model by modifying the stress-strain curve at unloading to an experimentally fitted quadratic curve.

The shear transfer model based on the contact surface density function[8] is used to consider the effect of shear stress transfer due to the aggregate interlock at the crack surface. The contact surface is assumed to respond elasto-plastically and the model is applicable to any arbitrary loading history. For unloading and reloading, the shear transfer model modified by the authors[4] is used.

3.2 Model for the reinforcing bars in concrete

The stress acting on the reinforcing bar embedded in concrete is not uniform and the value is maximum at locations where the bar is exposed to a crack plane. The constitutive equations for the bare bar may be used if the stress strain relation is in the elastic range. The post-yield constitutive law for the reinforcing bar in concrete considers the bond characteristics and the model is a bilinear model. Kato's model[9] for the bare bar under the reversed cyclic loading and the assumption of stress distribution denoted by a cosine curve were used to derive the mechanical behavior of reinforcing bars in concrete under the reversed cyclic loading.

3.3 Model for the prestressing tendons in concrete

Bilinear diagrams used to characterize the mild steel behavior, showing a brusque yielding, are not immediately extrapolable to prestressing tendons. For prestressing tendons, which does not have a definite yield point a multilinear approximation may be required. High strength

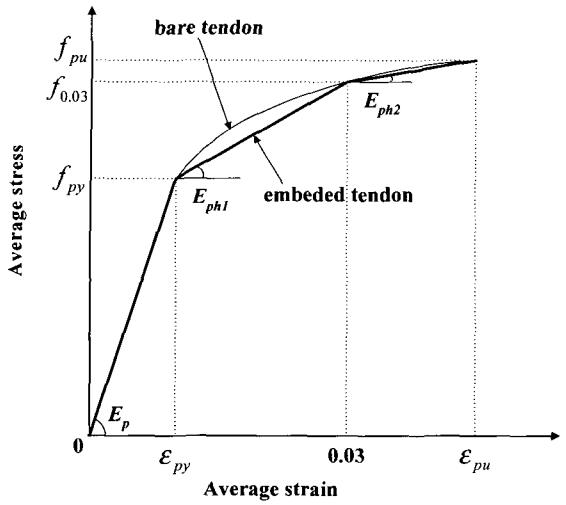

Fig. 4 Model for bonded tendons

steel used for prestressing shows a rather large proportional behavior followed by a progressive yielding. To simulate such a behavior, Kang[10] and Mari[11] used a multilinear diagram of five branches. In this study, the modified modeling is adopted for the present formulation as follows (see Fig. 4).

A trilinear model for the stress-strain relationship of prestressing tendon has been used. Unloading and reloading processes are accounted for through straight branches with the initial modulus.

$$\sigma_{pt} = f_{py} + E_{ph1}(0.03 - \varepsilon_{py}) + E_{ph2}(\varepsilon_{pu} - 0.03) \quad (1)$$

$$E_{ph1} = \frac{f_{0.03} - f_{py}}{0.03 - \varepsilon_{py}} \quad (2)$$

$$E_{ph2} = \frac{f_{pu} - f_{0.03}}{\varepsilon_{pu} - 0.03} \quad (3)$$

where σ_{pt} = stress of tendon; f_{py} = yielding strength of tendon; f_{pu} = ultimate strength of tendon; ε_{py} = yielding strain of tendon; ε_{pu} = ultimate strain of tendon; and E_{ph1}, E_{ph2} =strain hardening rates of the tendon embedded in concrete.

4. Modeling of the time dependent behavior

Concrete is unique among structural materials in that it undergoes complex physical and chemical changes over time, resulting in deformations and constitutive properties which are time dependent under practical service condition. Accurate consideration of time dependent concrete behavior is necessary for the accurate prediction of stresses and deflections in the structure at all load levels.

For the quasi-static time-dependent analysis, the time domain is divided into a discrete number of intervals, and a step-forward integration is performed in which increments of displacements, strains and stressed are successively added to the previous totals as the solution progresses in the time domain. At each time step, a direct stiffness analysis based on the displacement method is performed in the space domain in which the equilibrium equations to be solved are necessarily nonlinear due to various material nonlinearities considered.

4.1 Time dependent effect

An important assumption in studying and predicting the time dependent behavior of concrete structures is that the total strain in the concrete may be considered as a superposition of several independent components caused by different phenomena.

The nonmechanical strains (ε^{nm}) are introduced and defined as the part of the total strains (ε), which are obtained in addition to that which would have obtained in an instantaneous analysis (ε^{m})

$$\varepsilon = \varepsilon^{m} + \varepsilon^{nm} \quad (4)$$

Formally, the nonmechanical strains (ε^{nm}) can be treated as the initial strains so that the equilibrium condition, as introduced by the virtual work equation.

The following individual contributions are considered as part of the nonmechanical strains: concrete creep (ε^{c}), concrete shrinkage (ε^{s}), concrete ageing (ε^{a}), and possible strains due to thermal effects (ε^{t}). Just as an approach, superposition is assumed thus neglecting their actual coupling

$$\varepsilon^{nm} = \varepsilon^{c} + \varepsilon^{s} + \varepsilon^{a} + \varepsilon^{t} \quad (5)$$

Creep and shrinkage strains (ε^{c} and ε^{s}) in concrete are influenced by a number of factors depending on the mix design, the loading history, and the environment. Ageing strain (ε^{a}) is a fictitious stress originated strain which can be defined as the decrease in mechanical strain over time due to the increase in elastic modulus of the concrete. Temperature strain (ε^{t}) is a non-stress originated strain defined as the deformation under temperature change.

4.2 Model for the creep of concrete

Creep of concrete presents one of the most complex numerical problems in the time dependent analysis of concrete structures. The main factors influencing the creep of concrete are compressive strength, age at loading, aggregate type, ambient relative humidity and temperature, the specimen size, and the stress history.

Improved creep analysis model developed by Kang[12] is incorporated. The creep data can be generated automatically by the program utilizing ACI recommendations[13]. The ACI recommendations are provided in the equation from required for computer analysis.

4.3 Model for the shrinkage of concrete

Shrinkage of concrete is due primarily to loss of water upon drying (drying shrinkage) and volume change due to carbonation (carbonation shrinkage). The main factors influencing the shrinkage of concrete are aggregate type, water-cement ratio, specimen size, and ambient relative humidity. The ACI recommendations[13] are also provided in the equation from required for computer analysis.

4.4 Model for the relaxation of prestressing tendon

As experimentally stated, tensioned steel shows a delayed decrease of force when the length of the tendon is kept constant. The magnitude of the force loss depends mainly on the initial stress level in the tendon and on the service temperature. A direct mathematic formulation developed by Magura et al.[14] and previously utilized by Kang[10] is adopted for the present work as well. The model uses the following experimental formula

$$\frac{\sigma_p}{\sigma_{pi}} = 1 - \frac{\log_{10} t}{c}\left[\frac{\sigma_{pi}}{\sigma_{py}} - 0.55\right], \quad \text{for } \frac{\sigma_{pi}}{\sigma_{py}} \geq 0.55 \tag{6}$$

where

σ_p = predicted final stress for an initial stress σ_{pi} and after t days; σ_{py}= steel yielding stress; and c = constant (10 for stress-relieved tendon, 45 for low-relaxation tendon).

5. Numerical examples

The presented formulation has been implemented into computer as an extension of the existing program RCAHEST(Reinforced Concrete Analysis in Higher Evaluation System Technology), previously developed for

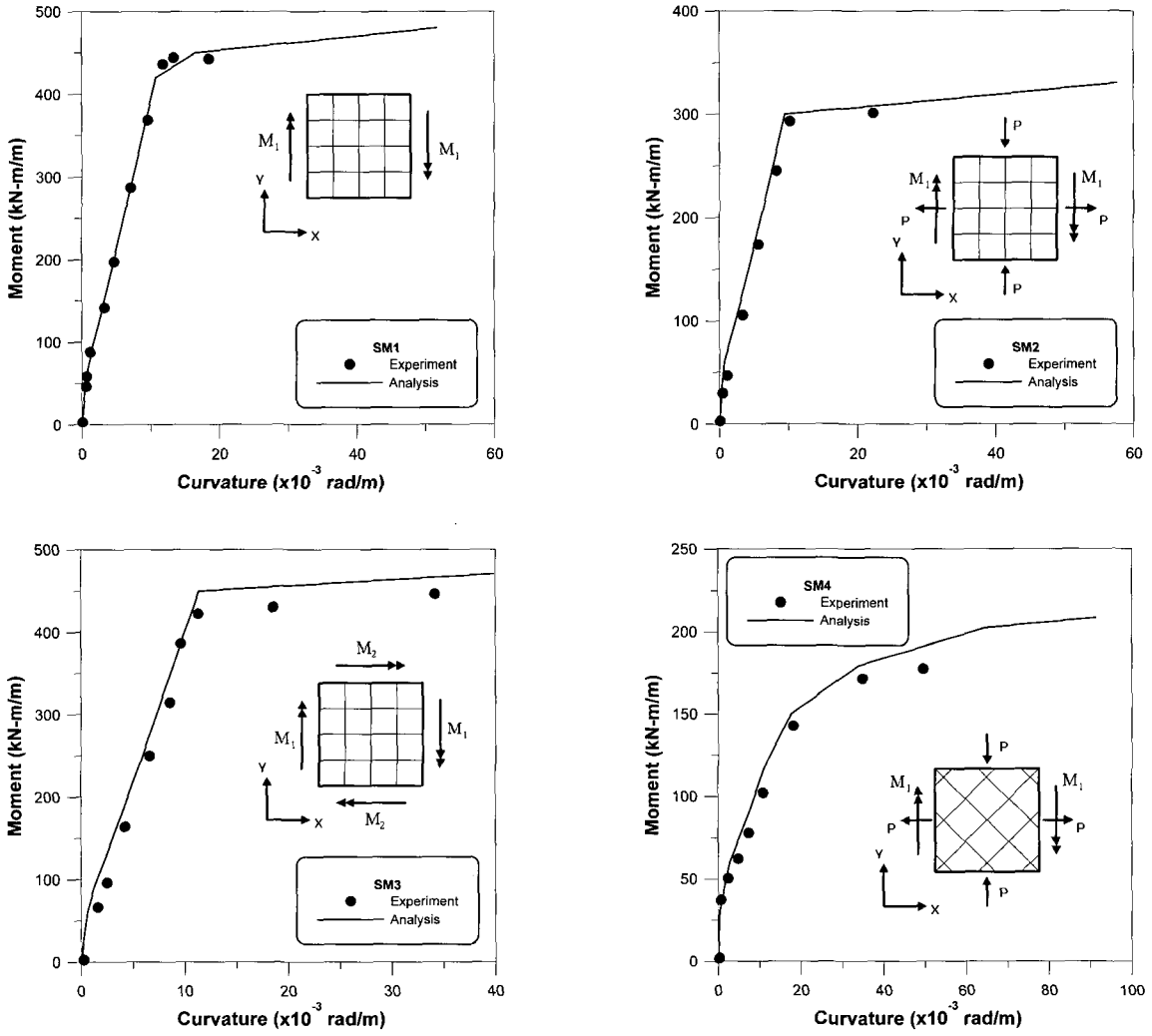

Fig. 5 Comparison of experimental and analytical responses

the nonlinear analysis of reinforced concrete structures[15]. The program is built around the finite element analysis program shell named FEAP, developed by Taylor[16]. Four numerical examples are presented through which, by comparison with existing experimental results, the efficiency and the reliability of the method are shown.

5.1 Reinforced concrete elements subjected to biaxial bending and in-plane loads

A series of tests by Polak[17] was used to verify the behavior of shell elements subjected to biaxial bending and in-plane loads. The specimens were the same size: 316 mm thick and 1,625 × 1,625 mm long, with effective test dimensions of 1,524×1,524 mm. All specimens contained reinforcement placed in two layers in each of the two orthogonal directions. Of particular interest was the influence of tension stiffening mechanisms; therefore, the reinforcement ratio in one direction was much higher than in the other direction. The specimen details and loading conditions are given in Table 1.

For finite element analysis, the specimens were modeled using a mesh of nine equal-sized elements. Ten layers per element were used for the integration through the depth.

Fig. 5 compares the analytical moment-curvature relations with the experimental results. In general, the results from the analysis were fairly accurate in predicting the behavior of specimens in terms of yield and ultimate moments. An exception was in the case of specimen SM4, where the prediction of ultimate moment was higher than the experimental result. Testing on this specimen was stopped because large deformation occurred in most of the panels before reaching final failure. Although, the predicted failure mode could not be directly compared with the observed one, the failure mode predicted by the analytical model was similar to the large deformation and flexural failure observed during the test.

5.2 Bouma's reinforced concrete shell

To verify the present analysis in a complete system made up of shell elements, the shells tested by Bouma et al[18]. were used as the basis for comparison. These shells, simply supported at the two ends and constructed of reinforced concrete, were 1/8-scale models of actual full-scale structures. As shown in Fig. 6, these scaled models had identical cross sections and edge beams but different span lengths and amounts of reinforcement. In this test series, load was proportionally increased until failure occurred.

Table 1 SM series test specimens

Spec.	Concrete	Reinforcement					Applied Loading
	f_c (MPa)	θ (deg)	ρ_x (%)	f_{xy} (MPa)	ρ_y (%)	f_{xy} (MPa)	M_1:M_2:P
SM1	47	0	1.25	425	0.42	430	1:0:0
SM2	62	0	1.25	425	0.42	430	0.25m:0:1
SM3	56	0	1.25	425	0.42	430	3.2:1:0
SM4	64	45	1.32	425	0.44	430	0.25m:0:1

The reinforcement details are shown in Fig. 7. Because the material data for the concrete and steel show substantial scattering in the tests, the mean values were adopted in this comparison study. The material properties are summarized as follows:

(1) Concrete: $f_c' = 28.4$ MPa, and $f_t = 4.9$ MPa; and

(2) Steel: $E_s = 206{,}153.3$ MPa, and $f_y = 294.4$ MPa.

Because of symmetry, the shell was modeled by 20 shell elements and 5 beam elements. The shell element was

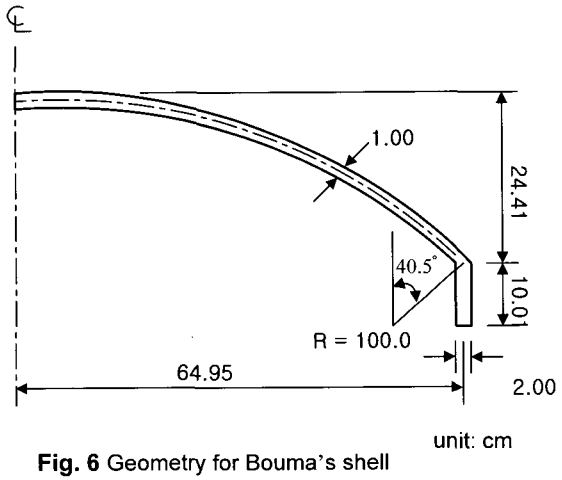

Fig. 6 Geometry for Bouma's shell

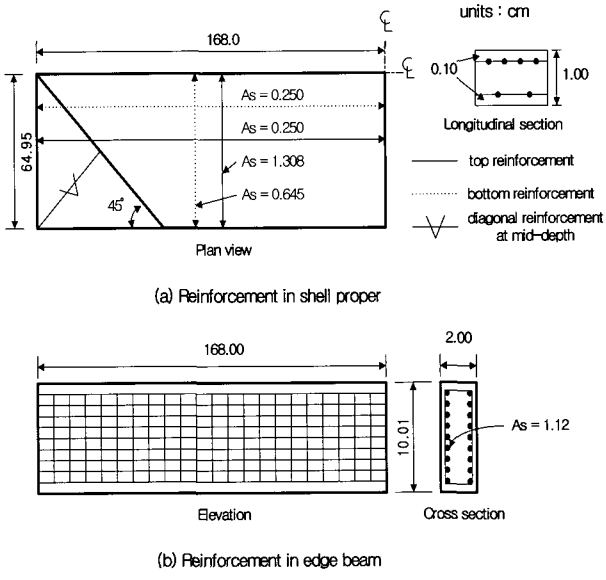

Fig. 7 Reinforcement layout for Bouma's shell

divided into 8 layers through the thickness. The resulting load-displacement response for the shell is presented in Fig. 8, together with test results by Bouma et al.[18] and the analytical results of two other studies[19,20]. The agreement between the present analytical results and the test results are satisfactory in terms of predicted strength and ductility.

5.3 Prestressed concrete elements subjected to in-plane shear force

Marti and Meyboom[21] conducted an experimental work in which panel specimens with partial prestressing were tested, as shown in Fig. 9. The three specimens were identical except for the reinforcement in one direction. In this direction, one specimen was nonprestressed while its two companion specimens were partially prestressed to various degrees. The main specimen properties are summarized in Table 2.

Because the force distribution is uniform across the element, only one finite element was used to predict the response of the specimen, and the number of layers used for per element was three. The resulting load-deformation response for specimens is presented in Fig. 10, together with test results and analytical results. It can be seen that the generation of cracks, yielding of steels, and ultimate strength were predicted with good agreements. An exception was in the case of specimen PP3, where the prediction of ultimate strength was lower than the experimental result. The satisfactory results of previous analysis by Marti and Meyboom[21] have been improved.

Compared to nonprestressed elements, prestressing results in higher cracking loads, reduced crack reorientation of the internal forces after cracking, delayed degradation of the concrete strength, lager strains in the reinforcement at ultimate, and higher ultimate loads.

5.4 Long-term behavior of the prestressed members

Table 2 Main specimen properties

Specimen		PP1	PP2	PP3
Prestress in x-direction (MPa)		0	2.07	4.40
Concrete	f_c' (MPa)	27.0	28.1	27.7
Reinforcement	ρ_{px} (%)	-	0.293	0.586
	f_{yp} (MPa)	-	910	910
	ρ_x (%)	1.492	1.295	0.647
	f_{yx} (MPa)	479	486	480
	ρ_z (%)	0.647	0.647	0.647
	f_{yz} (MPa)	480	480	480

The objectives of the selected experimental program[22] are to check the accuracy of the constitutive modeling for time-dependent analysis of prestressed concrete shells in this study. Prestressed concrete beams were cast to investigate the long-term behavior of the prestressed members under effects of creep and shrinkage. These specimens, with dimensions of 15 cm × 20 cm × 400 cm, were cast in the laboratory as shown in Fig. 11.

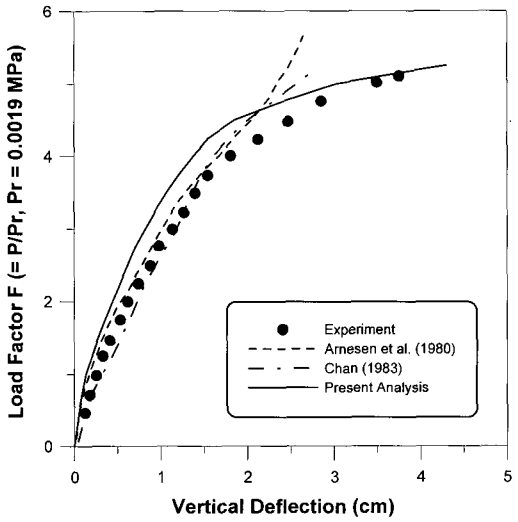

Fig. 8 Load-deflection curves at midspan of edge beam

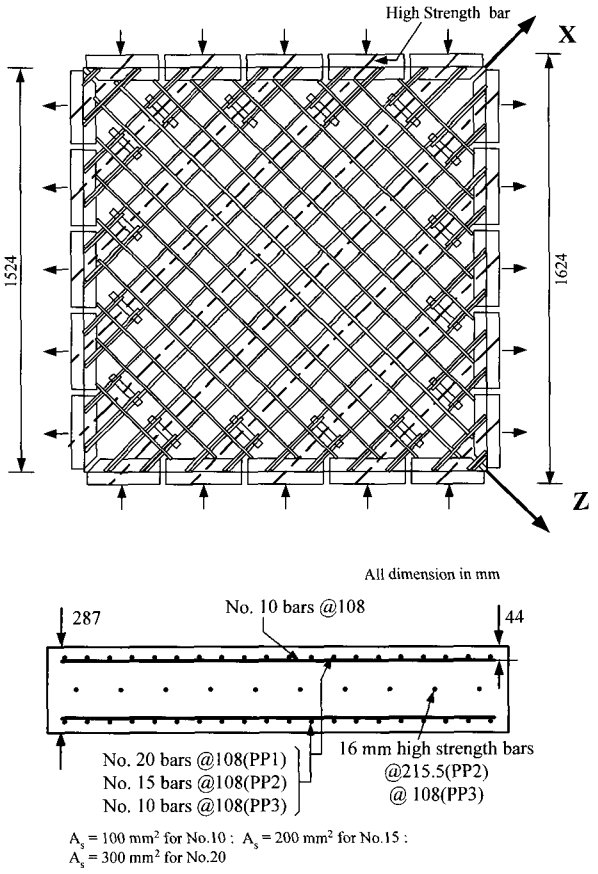

Fig. 9 Application of stresses of specimens and reinforcement layout

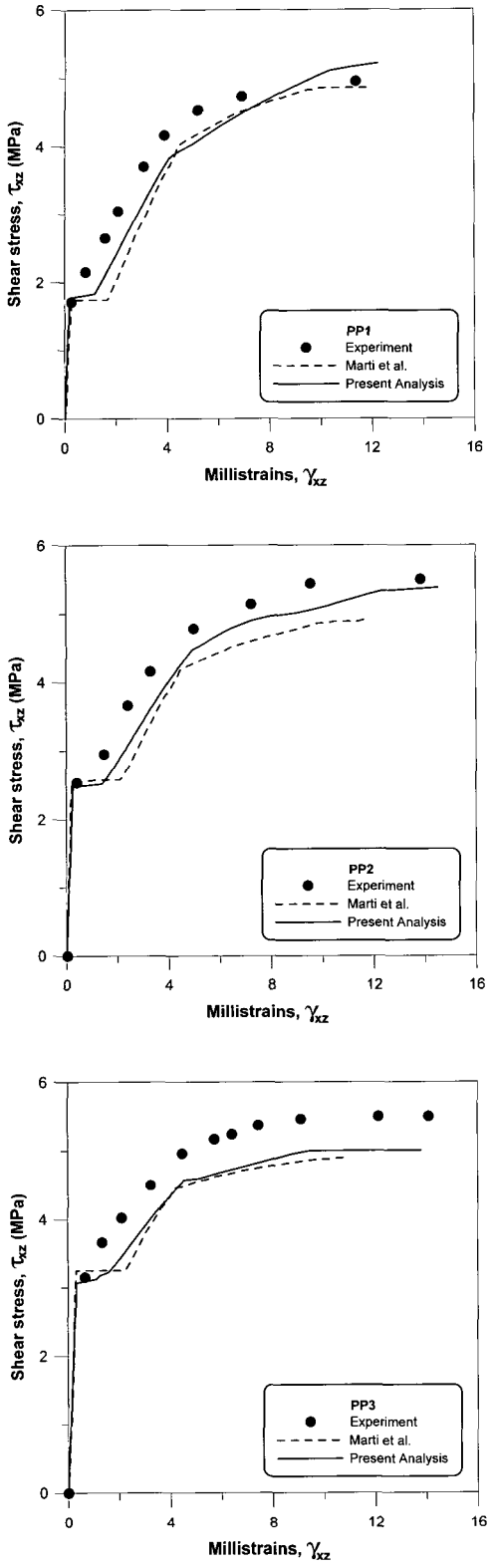

Fig. 10 Predicted and measured load-deformation response

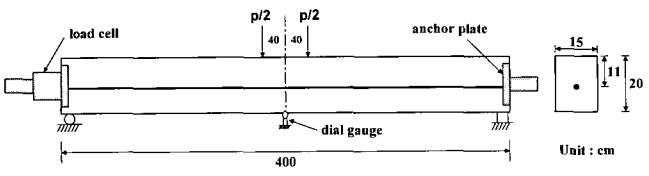

Fig. 11 Flexural test setup

Table 3 Modulus of elasticity and compressive strength

Age of test (day)	Cylinder strength f_c' (kgf/cm^2)	Modulus of elasticity E_c (10^5 kgf/cm^2)
3	279	1.95
7	344	2.24
28	466	2.40

Note: 1 kgf/cm^2 = 0.098 MPa.

Table 4 Material property of prestressing tendon

Diameter (mm)	Area of section (mm^2)	Yield loading (kgf)	Failure stress (kgf/cm^2)	Rate loss(%)	Unit weight (kgf/km)
12.83	100.27	17,688	19,699	0.54	780

Note: 1 kgf = 9.80665 N; 1 kgf/cm^2 = 0.098 MPa.

Table 5 Parameters of flexure experiment

Specimen	Initial prestress(kgf)	Age (day)	Loading (kgf)	Factor	
				Creep	Shrinkage
SB03B	-	3	-	Yes	Yes
SB13B	9,926	3	293	Yes	Yes
SB13C	10,269	3	292	Yes	No
SB17B	10,999	7	292	Yes	Yes

Note: 1 kgf = 9.80665 N.

The prestressing tendons were straight and located 11 cm from the top face of the beam. The material properties of the specimens are listed in Tables 3 and 4.

This experiment consisted of four specimens. The fist one was the control specimen which was not subjected to any loading and prestress (SB03B). The second and the third ones were subjected to the prescribed loading and prestress (SB13B, SB13C). The last specimen was the same as SB13B except for the loading age of 7 day (SB17B). Additionally, in order to understand the behavior of unloading and recovery, specimen SB17B was unloaded after 117 day. The parameters for each specimen were summarized in Table 5.

This analysis modeled the specimens using mesh of 10 elements. The shell element was divided into 10 layers through the thickness. The comparison between analytical and experimental results is shown in Fig. 12 (a) to (d). The analytical results show a good agreement with the experimental results, not only in regards to loading, but also in unloading.

6. Conclusions

A nonlinear finite element procedure for the analysis of reinforced and prestressed concrete shells was developed based on the four-node quadrilateral flat shell element with drilling rotational stiffness. In order to analyze reinforced

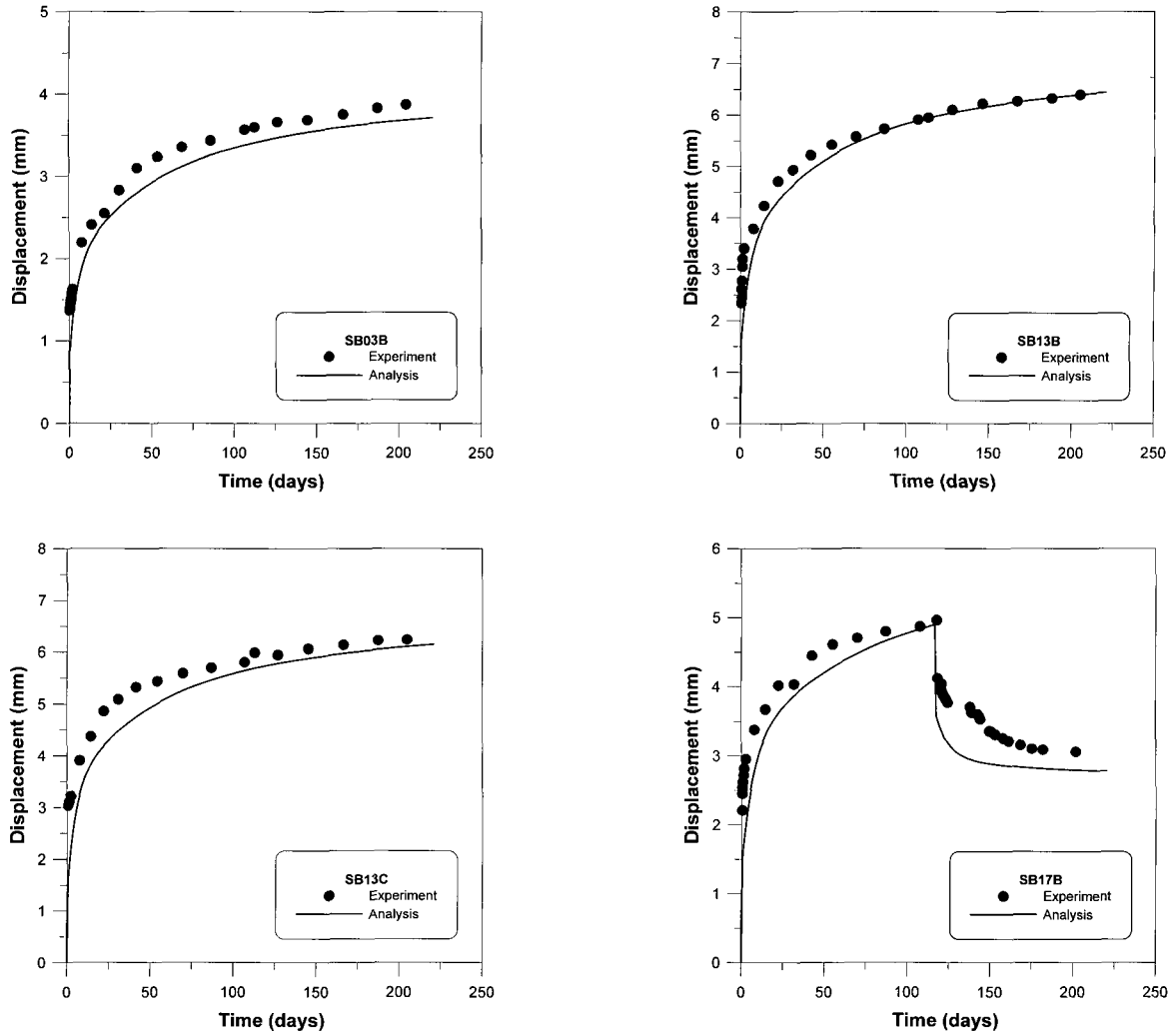

Fig. 12 Displacement at the middle of beam versus time

and prestressed concrete shell with nonlinear behavior, this study introduces the layer method, which assumes that several thin plane stress elements are layered in the direction of thickness. The analysis takes into account material nonlinearity by incorporating tensile, compressive and shear models of cracked concrete, in addition to including a model for the reinforcing steel and tendon. Prestressing is considered as an internal force on the element. This consistency, together with some practical implementation considerations, make it possible to use the proposed formulation to include the numerical treatment of prestressing in many existing numerical models previously developed for reinforced concrete shells.

Because the general shell element has 5-DOFs, it was necessary to introduce a degree of freedom in the direction of member rotation to combine with three-dimensional beam-column element with 6-DOFs. Thus, the developed element in this study is promising for broader application in the analysis of general structures consisting of slab, shear wall, and beam-column.

The results obtained with the numerical model in the case of four examples of application are presented and compared with experimental and analytical results from other authors. Through those examples, the capability of the numerical model to realistically represent the nonlinear behavior of reinforced and prestressed concrete shells throughout their initial, cracked and ultimate ranges is shown. However, some are detected that require further experimental and theoretical research. The resulting presented program has proved to be very effective in clarifying the structural behavior under increased and sustained loads. It can be used in structural analysis or as a powerful research tool, complementing experimental investigations, for defining more precise practical rules to be adopted in the design of reinforced and prestressed concrete shell structures.

Acknowledgements

The study described in this paper was supported by the Ministry of Construction and Transportation through the Korea Bridge Design and Engineering Research Center. The authors wish to express their gratitude for the support received.

References

1. Roca, P. and Mari, A. R., "Nonlinear Geometric and Material Analysis of Prestressed Concrete General Shell Structure", *Computers & Structures*, Vol.46, No.5, 1993, pp.917~929.
2. ACI, *Finite Element Analysis of Reinforced Concrete Structures*, ACI, 2001, 399 pp.
3. Polak, M. A. and Vecchio, F. J., "Nonlinear Analysis of Reinforced Concrete Shells", *Journal of Structural Engineering*, ASCE, Vol.119, No.12, 1993, pp.3439~3462.
4. Kim, T. H., Lee, K. M., and Shin, H. M., "Nonlinear Analysis of Reinforced Concrete Shells using Layered Elements with Drilling Degree of Freedom", *ACI Structural Journal*, Vol.99, No.4, 2002, pp.418~426.
5. Roca, P. and Mari, A. R., "Numerical Treatment of Prestressing Tendons in the Nonlinear Analysis of Prestressed Concrete Structures", *Computers & Structures*, Vol.46, No.5, 1993, pp.905~916.
6. Maekawa, K. and Okamura, H., "The Deformational Behavior and Constitutive Equation of Concrete Using Elasto-Plastic and Fracture Model", *Journal of the Faculty of Engineering*, University of Tokyo, Vol.37, No.2, 1983, pp.253~328.
7. Shima, H., Chou, L., and Okamura, H., "Micro and Macro Models for Bond Behavior in Reinforced Concrete", *Journal of the Faculty of Engineering*, University of Tokyo, Vol.39, No.2, 1987, pp.133~194.
8. Li, B. and Maekawa, K., "Contact Density Model for Stress Transfer across Cracks in Concrete", *Concrete Engineering*, JCI, Vol.26, No.1, 1988, pp.123~137.
9. Kato, B., "Mechanical Properties of Steel under Load Cycles Idealizing Seismic Action", *CEB Bulletin D'Information*, Vol.131, 1979, pp.7~27.
10. Kang, Y. J., *Nonlinear Geometric, Material and Time Dependent Analysis of Reinforced and Prestressed Concrete Frames*, University of California, Berkeley, UC-SESM Report No.77-1, 1977, 243pp.
11. Mari, A. R., *Nonlinear Geometric, Material and Time Dependent Analysis of Three Dimensional Reinforced and Prestressed Concrete Frames*, University of California, Berkeley, UC-SESM Report No.84-12, 1984.
12. Kang, Y. J., *SPCFRAME - Computer Program for Nonlinear Segmental Analysis of Planar Prestressed Concrete*, University of California, Berkeley, UC-SESM Report No.89-07, 1989, 115pp.
13. ACI Committee 209, *Prediction of Creep, Shrinkage and Temperature Effects in Concrete Structures*, ACI209R-92, 1992.
14. Magura, D. D., Sozen, M. A., and Seiss, C. P., "A Study of Stress Relaxation in Prestressing Reinforcement", *PCI Journal*, Vol.9, No.2, 1964, pp.13~57.
15. Kim, T. H. and Shin, H. M., "Analytical Approach to Evaluate the Inelastic Behaviors of Reinforced Concrete Structures under Seismic Loads", *Journal of the Earthquake Engineering Society of Korea*, EESK, Vol.5, No.2, 2001, pp.113~124.
16. Taylor, R. L., *FEAP - A Finite Element Analysis Program, Version 7.2 Users Manual, University of California, Berkeley*, Vol.1 and Vol.2, 2000, 379pp.
17. Polak, M. A., *Nonlinear Analysis of Reinforced Concrete Shells*, PhD Thesis, University of Toronto, Toronto, Canada, 1992, 195pp.
18. Bouma, A. L., Van Riel, A. C., Van Koten, H., and Beranek, W. J., *Investigations of Models of Eleven Cylindrical Shells Made of Reinforced and Prestressed Concrete*, Symposium on Shell Research, Delft, 1961.
19. Arnesen, A., Soresen, S. I., and Bergan, P. G., " Nonlinear Analysis of Reinforced Concrete", *Computers & Structures*, Vol.12, 1980, pp.571~579.
20. Chan, E. C., *Nonlinear Geometric, Material and Time Dependent Analysis of Reinforced Concrete Shells with Edge Beams*, PhD Dissertation, Divisions of Structural Engineering and Structural Mechanics, University of California, Berkeley, Calif., UC-SESM Report No.82-8, 1983.
21. Mari, P. and Meyboom, J., "Response of Prestressed Concrete Elements to In-Plane Shear Forces", *ACI Structural Journal*, Vol.89, No.5, 1991, pp.503~514.
22. Chiu, H. S., Chern, J. C., and Chang, K. C., "Long-Term Deflection Control in Cantilever Prestressed Concrete Bridges Ⅱ: Experimental Verification", *Journal of Engineering Mechanics*, ASCE, Vol.122, No.6, 1996, pp. 495-501.